AlInAsSb Single-Photon Avalanche Photodiodes

Joe C. Campbell*[a] and Kubra Circir[a]
[a]Department of Electrical and Computer Engineering, University of Virginia, Charlottesville, Virginia 22903, USA *jcc7s@virginia.edu

ABSTRACT

A key parameter for avalanche photodiodes (APDs) used in quantum optics is single-photon detection efficiency, which is expressed as a product of external quantum efficiency and the avalanche breakdown probability. APDs with disparate electron and hole ionization coefficients, described by their ratio, k, are predicted to achieve higher avalanche breakdown probabilities. Recently, it has been shown that Sb-containing III-V compound semiconductors such as AlInAsSb and AlGaAsSb exhibit very low k values, typically less than 0.05, indicating a high breakdown probability. This is confirmed in this paper, which reports AlInAsSb/InGaAs single-photon avalanche diodes reaching breakdown probabilities as high as 90%.

Keywords: Photodetector, avalanche photodiode, single photon detection

1. INTRODUCTION

Recently, the rapid emergence of quantum optics for quantum communications, signal processing, and next-generation computing has generated expectations of imminent technological breakthroughs. However, many of the necessary components do not yet meet the required performance standards, or practical implementations are still unavailable. This is especially true for one of the key components, single-photon detectors, where higher detection efficiency and photon-number resolution (PNR) are critical. We present a new method to achieve high detection efficiencies in single-photon avalanche diodes (SPADs). Currently, the most common types of single-photon detectors are superconducting nanowire single-photon detectors (SNSPDs) and single-photon avalanche diodes (SPADs. At cryogenic temperatures, SNSPDs have demonstrated excellent performance, with photon detection efficiency (PDE) exceeding 90%, dark count rates below 0.01 cps, timing jitter as low as 2.6 ps, and dead times compatible with gigahertz photon-count rates. SPADs, on the other hand, can operate at higher temperatures, including room temperature, which is an advantage over SNSPDs, which require cryogenic cooling. However, a major challenge for SPADs is achieving very high PDE values, which are essential for some quantum optics applications such as quantum computing. The photon detection efficiency of a SPAD can be expressed as PDE = $\eta_{EQE} \times P_{avalanche}$, where η_{EQE} is the external quantum efficiency at unity gain and $P_{avalanche}$ is the avalanche breakdown probability. In simple terms, η_{EQE} is the likelihood that a photon creates an electron-hole pair that moves toward the electrodes, and $P_{avalanche}$ is the likelihood that the generated electron or hole triggers a self-sustaining avalanche, or breakdown.

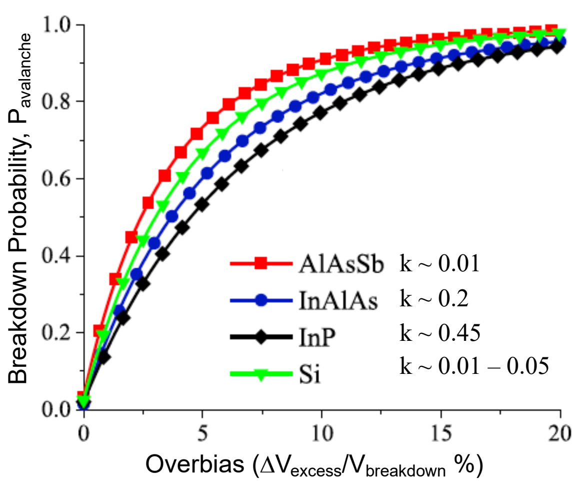

Figure 1. Avalanche breakdown probability, $P_{avalanche}$, versus excess bias for AlAsSb, InAlAs, InP, and Si after Ref. [1].

It has been shown that APDs with low k values have higher breakdown probabilities for a given excess-bias level [1]. This is illustrated in Fig. 1, which shows $P_{avalanche}$ versus excess bias for AlAsSb, InAlAs, InP, and Si [2]. The most widely used SPADs in the infrared use an InGaAs absorber with an InP multiplication region. Signorelli reported InP/InGaAs SPADs designed for high PDE. A 2 µm-thick InGaAs absorber and an anti-reflection coating produced a QE of 75% [3]. However, the PDE was 50% since $P_{avalanche}$ ~ 0.67. Higher QE can be achieved with thick InGaAs absorbers [4] or a waveguide structure. In theory, InP can reach a $P_{avalanche}$ of around 100% for sufficiently high excess bias. However, in practice, the excess bias needed for this results in unacceptably high dark counts and increased afterpulse rates. The excess noise of InP is characterized by a relatively high k value of 0.45. Conversely, Si exhibits intrinsically low excess noise, with a k value of 0.01 [5, 6]. Recently, a room-temperature Si-based SPAD has been reported [7]. The structure combines a Ge absorption layer to extend responsivity into the infrared with a Si multiplication region to achieve low-noise characteristics. At 1.3 µm wavelength, the PDE and $P_{avalanche}$ were 12% and 0.5, respectively. Previously, we demonstrated APDs in a new material system, AlInAsSb, with very low excess noise ($k < 0.05$) in linear-mode operation [8]. In this paper, we report on AlInAsSb SPADs with a PDE of 52% and an avalanche breakdown probability as high as 90%.

2. AlInAsSb AVALANCHE PHOTODIODES

The III-V compound quaternary $Al_xIn_{1-x}As_ySb_{1-y}$ has material characteristics that make it attractive for low-noise linear-mode APDs and high-detection-efficiency SPADs. The equivalent bandgap energy can be tuned from approximately 1 µm to 5 µm by adjusting the Al concentration, which can be used to design APDs that operate from the visible to the mid-wavelength spectrum. Going forward, $Al_xIn_{1-x}As_ySb_{1-y}$ will be referred to by its Al concentration as Al_xInAsSb.

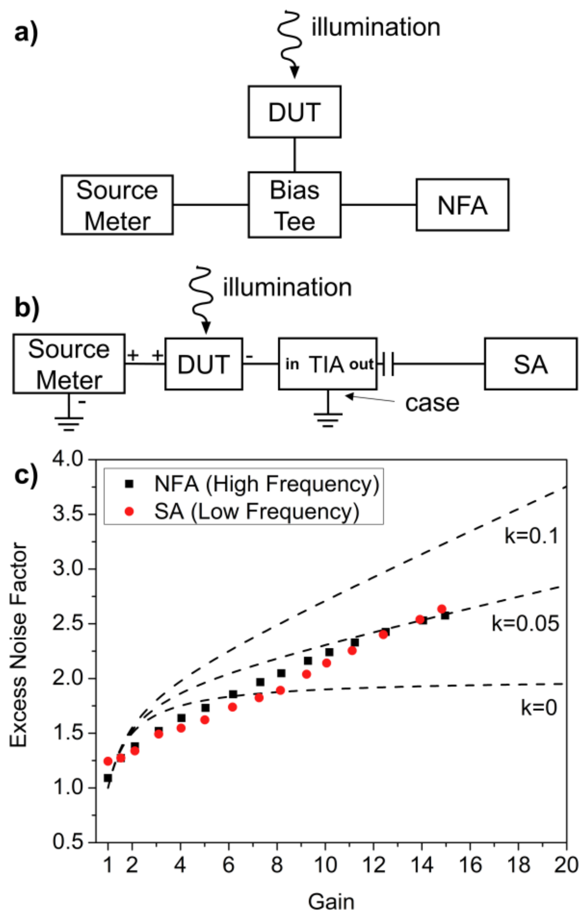

Figure 2. (a) The noise-figure-analyzer-based setup for measurements above 10 MHz. (b) The spectrum-analyzer-based setup for measurements between ~20 kHz and ~400 kHz. (c) The excess noise factor versus gain for a 100-µm diameter $Al_{0.7}$InAsSb PIN using the two different setups in (a) and (b).

Excess noise factor measurements were carried out using two setups [9]. The first measured the excess noise factor above 10 MHz with an Agilent 8973 Noise Figure Analyzer (NFA). The second method, designed by Leonardo DRS, Inc., allows measurements at frequencies as low as approximately 20 kHz using a low-noise transimpedance amplifier and an Agilent E4440A spectrum analyzer (SA). Block diagrams of these setups are shown in Figures 2(a) and 2(b). The two measurements are plotted in Fig. 2(c). The difference is no more than 8%.

3. AlInAsSb SINGLE-PHOTON AVALANCHE DIODES

Figure 3 shows the epitaxial layer structure of an Al0.79InAsSb Separate Absorption, Charge, and Multiplication (SACM) SPAD and the electric field profile after punch-through. The structure was grown on a semi-insulating InP substrate using molecular beam epitaxy. Highly doped InGaAs layers were added at the top and bottom of the SACM structure as contact layers. The multiplication region is Al0.79InAsSb, and the absorber is InGaAs. Between the multiplication region and the InGaAs absorber, the bandgap is continuously graded to prevent charge trapping at the interface [11]. Mesa structures were etched through standard photolithography and wet etching in citric acid, phosphoric acid, hydrogen peroxide, and water. The mesa sidewalls were passivated by spinning and patterning a 500 nm thick layer of SU-8 photoresist.

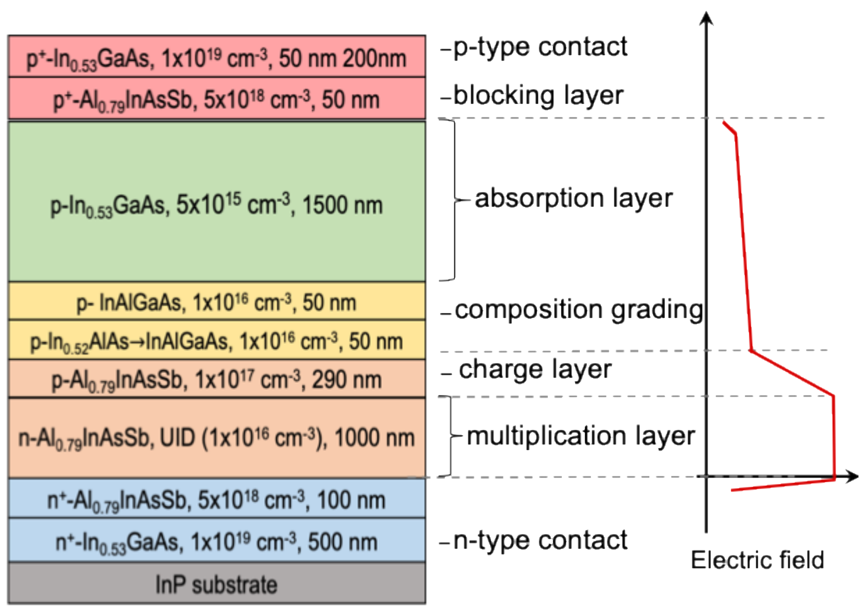

Figure 3. Schematic cross section of $Al_{0.79}InAsSb/InGaAs$ SACM APD and electric field profile..

Figure 4 shows the photocurrent and dark current of a 150 µm-diameter $Al_{0.79}InAsSb/InGaAs$ SACM SPAD at 200K. These SPADs were designed to have the punch-through near the breakdown voltage to reduce the electric field in the absorber, thus decreasing dark current and dark counts.

To accurately determine the avalanche breakdown probability, it is essential to obtain a precise value for the unity-gain external quantum efficiency (EQE). For SACM structure APDs, this becomes complicated if there is gain at punch-through, which depends on the doping level in the charge layer. In such cases, responsivity is given by the product of quantum efficiency and avalanche gain. We employed three methods to estimate the quantum efficiency. First, the electric field profile was calculated for voltages above the punch-through using the CHARGE solver in ANSYS Lumerical simulation software. Next, the field dependence of the ionization coefficients was used to determine the gain [12,13,14], and the efficiency was derived from the measured responsivity. This approach yielded an EQE of 55%. A wafer similar to the one shown in Fig. 4, but with lower charge-layer doping, was used for the other two methods. For this wafer, the punch-through voltage was 45 V, with a flat photocurrent region extending a few volts above the punch-through voltage. A power meter measured the input optical signal level within the flat photocurrent region. The EQE determined by this method was 57%. Lastly, the spectral response was measured using a tungsten-halogen light source, a spectrometer, a lock-in amplifier, and a calibrated $In_{0.53}Ga_{0.47}As$ PIN photodiode. The EQE found was 55%. We note that the absorption layer is only 1 µm thick, there is no anti-reflection coating, and the structure is such that photons make a single pass across the absorber, meaning there is no "back reflection." Higher detection efficiency can be achieved by using thicker InGaAs absorption layers and adding an anti-reflection coating on the top surface.

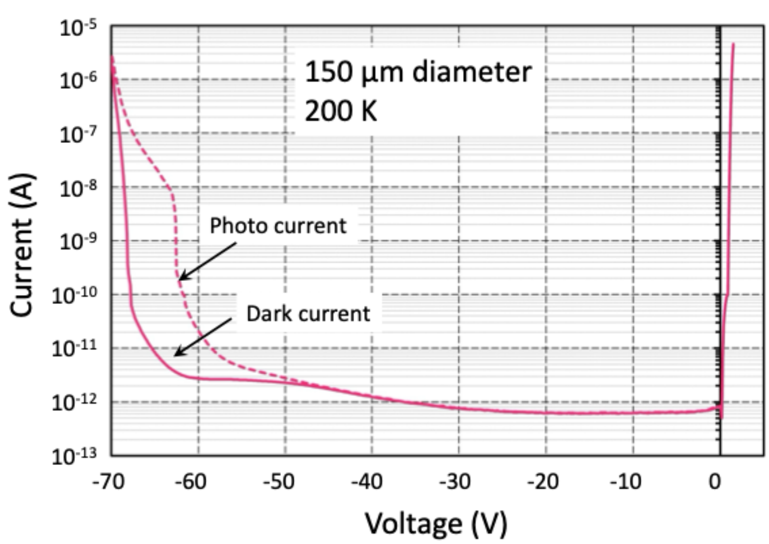

Figure 4. Photocurrent and dark current of 150 µm-diameter $Al_{0.79}InAsSb/InGaAs$ SACM APDs

The gated-quenching circuit used for single-photon characterization has been described in a previous work [15]. The over-bias level was set by applying square gate pulses with rise and fall times of 100 ps and a width of 5 ns at a repetition rate of 10 kHz. A 1550 nm DFB laser was coupled into a cryochamber using a single-mode optical fiber and connected to the front surface of the SPAD through a cleaved fiber. The fiber was aligned by illuminating the SPAD while biased above its punch-through voltage and then maximizing the photocurrent. A digital variable optical attenuator (VOA) was used to reduce the optical power level to 0.1 photons per pulse. A PicoQuant HydraHarp 400 counter was used to measure count statistics, with the discriminator level set to the lowest voltage possible without counting from the circuit's capacitive transients.

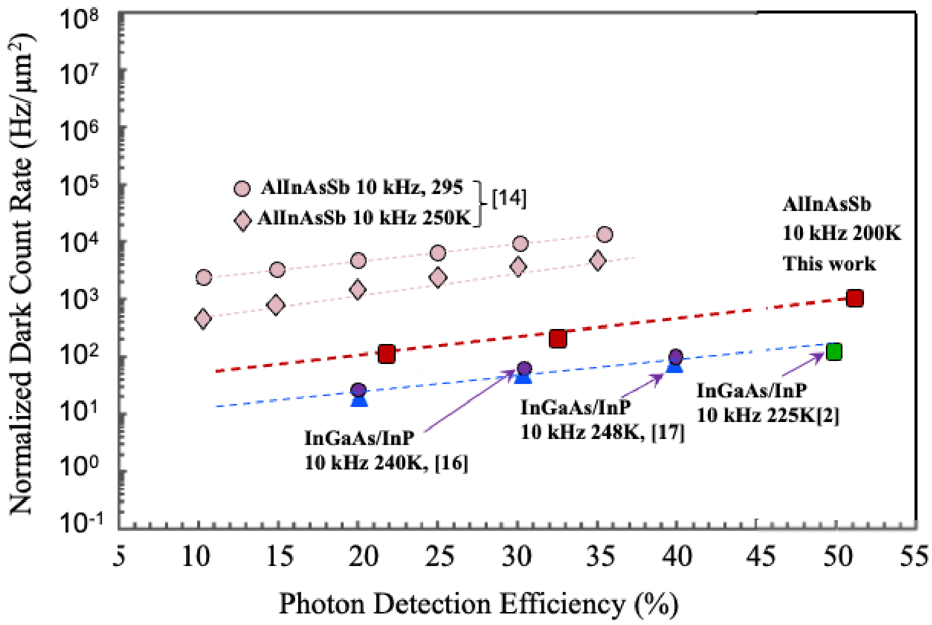

Figure 5. Normalized dark count rate versus photon detection efficiency of $Al_{0.79}InAsSb$ SACM SPAD 200K. Also shown are state-of-the-art results for InP/InGaAs SPADs [1,16,17]

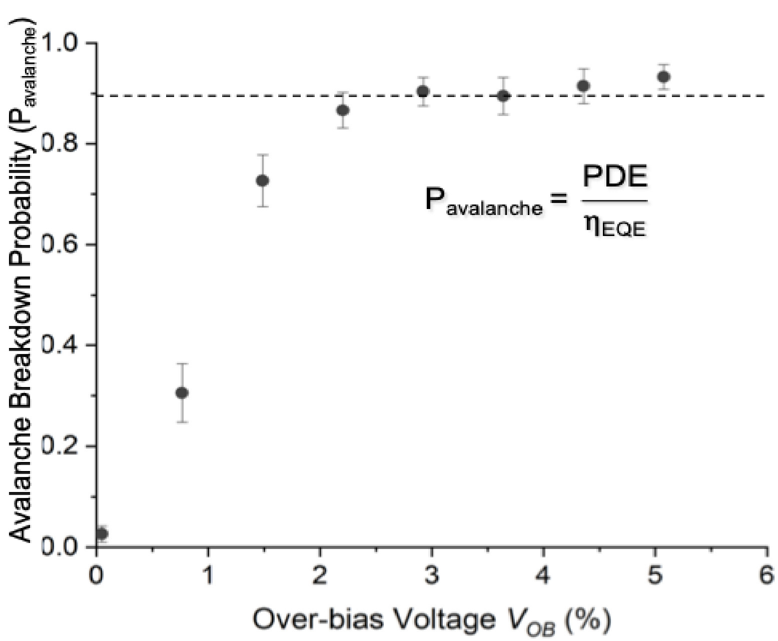

Figure 6. Average avalanche breakdown probability versus over bias voltage.

The normalized dark count densities at 295 K, 250 K, and 200 K (this work) are plotted in Fig. 5 as a function of photon detection efficiency. Also included are state-of-the-art results for InP/InGaAs SPADs [2,16,17]. The highest single-photon detection efficiency reaches 52%, which is comparable to the best InP/InGaAs SPADs; however, the dark counts are significantly higher. This may be due to the more mature InP material technology or the fact that Al compounds grown by molecular beam epitaxy are prone to oxygen impurities. Growth techniques that have successfully reduced defect levels in other materials, such as changing substrate orientation or adjusting the cracking temperature for the column V elements, are currently being investigated.

The avalanche breakdown probability was calculated using the external quantum efficiency and PDE measurements shown in Figure 5. Figure 6 shows the average $P_{avalanche}$ values for six $Al_{0.79}InAsSb$ SACM SPADs as a function of over-bias voltage. The measured $P_{avalanche}$ rises rapidly with over-bias, reaching an average of 90 ± 3% at an over-bias of 3%, the highest value reported to date.

CONCLUSIONS

In conclusion, the single-photon characteristics of an $Al_{0.79}InAsSb/InGaAs$ SACM SPAD were demonstrated, achieving a photon detection efficiency of 52%. The low k value of the $Al_{0.79}InAsSb$ multiplication layer allowed an avalanche breakdown probability as high as 90% at an over-bias level of 3%. These results offer a pathway toward single-photon detection efficiencies approaching 100% at moderate cryogenic temperatures. Furthermore, the moderate-temperature operation of this III-V compound SPAD is an important step toward integrated waveguide-coupled SPADs as components in photonic integrated circuits.

ACKNOWLEDGEMENTS

This work was supported by the DARPA INSPIRED program (HR0011-24-2-0360) and the National Science Foundation (2533557).

REFERENCES

[1] Dautet, H., Deschamps, P., Dion,B., MacGregor, A. D., MacSween, D., McIntyre, R. J., Trottier, C. and Webb, P. P. "Photon counting techniques with silicon avalanche photodiodes," Appl. Opt., vol. 32, no. 21, pp. 3894–3900, Jul. 1993.

[2] Ahmed, J., Xie, S., Liang, B., Yi, X., Jin, X., Kesaria, M., David, J. P. R., and Huffaker, D. L., "Theoretical Analysis of AlAs0.56Sb0.44 Single Photon Avalanche Diodes with High Breakdown Probability," IEEE J. Quant. Electron., vol 57, no. 2, 4500206, April 2021.

[3] Signorelli, F., Telesca, F., Conca, E., Della, F., Ruggeri, A., Giudiec, A., and Tosi, A., "InGaAs/InP SPAD detecting single photons at 1550 nm with up to 50 % efficiency and low noise," 2021 IEEE International Electron Devices Meeting (IEDM), p 4, 2021.

[4] Shen, Y., Xue, X., Jones, A. H., Peng, Y., Gao, J., Tzu, T. C., Konkol, M., and Campbell, J. C., "Near 100% external quantum efficiency 1550-nm broad spectrum photodetector," Opt. Express, vol. 30, no. 2, pp. 3047-3054, January 17, 2022

[5] Webb, P. P., McIntyre, R. J., and Conradi, J., "Properties of avalanche photodiodes," RCA Review, vol. 35, no. 2, pp. 234-278, 1974.

[6] Robbins, V. M., Wang, T., Brennan, K. F., Hess, K., and Stillman, G. E., "Electron and hole impact ionization coefficients in (100) and in (111) Si," J. Appl. Phys., vol. 58, pp. 4614-4617, 1985.

[7] Na, N., Hsu, C.-Y., and Soref, R., "Room temperature operation of germanium–silicon single-photon avalanche diode," Nature, vol. 627, p. 295, March 14, 2024.

[8] Ren, M., Maddox, S. J., Woodson, M. E., Chen, Y., Bank, S. R., and Campbell, J. C., "Characteristics of $Al_xIn_{1-x}AsySb1-y$ (x:0.3–0.7) avalanche photodiodes," J. Lightwave Technol., vol. 35, no. 12, pp. 2380–2384, Jun. 2017.

[9] Jones, A. H., March, S. D., Bank, S. R., and Campbell, J. C., "Low-noise high-temperature AlInAsSb/GaSb avalanche photodiodes for 2-μm applications," Nat. Photonics, vol. 14, no. 9, pp. 559–563, 2020.

[10] Ronningen, T. J., Kodati, S. H., Jin, X., Lee, S., Jung, H., Tao, X., Lewis, H. I. J., Schwartz, M., Gajowski, N., Martyniuk, P., Guo, B., Jones, A. H., Campbell, J. C., Grein, C., David, J. P. R., and Krishna, S., "Ionization coefficients and excess noise characteristics of AlInAsSb on an InP substrate," Appl. Phys. Lett., vol. 123, no. 13, p. 131110, September 25, 2023.

[11] Yuan, Yuan, Rockwell, A. K., Peng, Yiwei, Zheng, Jiyuan, March, S. D., Jones, A. H., Ren, Min, Bank, S. R., and Campbell, J. C., "Comparison of Different Period Digital Alloy Al0.7InAsSb Avalanche Photodiodes," J. Lightwave Tech., vol. 37, no. 14, pp. 3647-3654 (15 July 2019).

[12] Yuan, Yuan, Zheng, Jiyuan, Tan, Yaohua, Peng, Yiwei, Rockwell, A. K., Bank, S. R., Ghosh, A. W., and Campbell, J. C., "Temperature dependence of the ionization coefficients of InAlAs and AlGaAs digital alloys," J. Photonics Research, vol. 6, no. 8, pp. 794-799, August 1, 2018.

[13] Herrera, D.J., Dadey, A.A., March, S.D., Bank, S. R., and Campbell, J. C., “AlInAsSb Geiger-mode SWIR and eSWIR SPADs with high avalanche probability,” Opt. Express, OE **32**(2), 2106–2113 (2024).
[14] Liu, Mingguo, Bai, Xiaogang, Hu, Chong, Guo, Xiangyi, Campbell, J. C., Pan, Zhong, and Tashima, M. M., **“**Low Dark Count Rate and High Single-Photon Detection Efficiency Avalanche Photodiode in Geiger-Mode Operation,” IEEE Photon. Tech. Lett., vol. 19, no. 6, pp. 378-380, March 15, 2007.
[15] Jiang, X., Itzler, M., O’Donnell, K. O., Entwistle, M., Ownes, M., Krystyna, S., and Sabbir, R.,"InP-Based Single-Photon Detectors and Geiger-Mode APD Arrays for Quantum Communications Applications," IEEE J. Sel. Top. Quant. Electron., vol. 21, no. 3, pp. 5-16, May-June 2015.